

# Stimulated reversal of the strong adhesion of catechol onto a silica surface

Muhammad Ilyas<sup>1</sup> | Shabeer Ahmad Mian<sup>1</sup> | Abdur Rauf<sup>2</sup> | Ejaz Ahmed<sup>3</sup> | Gul Rahman<sup>4</sup> | Arindam Sanyal<sup>5</sup> | Joonkyung Jang<sup>5</sup> 

<sup>1</sup>Department of Physics, University of Peshawar, Peshawar, Pakistan

<sup>2</sup>Department of Physics, Islamia College University, Peshawar, Pakistan

<sup>3</sup>Department of Physics, Abdul Wali Khan University, Mardan, Pakistan

<sup>4</sup>Institute of Chemical Sciences, University of Peshawar, Peshawar, Pakistan

<sup>5</sup>Department of Nanoenergy Engineering, Pusan National University, Busan, South Korea

## Correspondence

Shabeer Ahmad Mian, Department of Physics, University of Peshawar, Peshawar, Pakistan.  
Email: shabeerahmad@uop.edu.pk

Joonkyung Jang, Department of Nanoenergy Engineering, Pusan National University, Busan, South Korea.  
Email: jkjang@pusan.ac.kr

## Funding information

Pusan National University

## Abstract

Marine mussels permanently adhere to various surfaces via catechol (1,2-dihydroxybenzene) functional groups. Such biofouling causes adverse effects, including the corrosion and dragging of a marine vessel. By using the density functional theory, we show an electrical stimulus detach a catechol molecule that strongly adhered to a silica surface. A moderate electric field significantly decreases the binding energy of catechol adhered to a dry or wet silica surface.

## KEYWORDS

catechol, desorption, electric stimulus, marine mussel, silica surface

## INTRODUCTION

*Fouling* refers to an undesirable adhesion of an organism or substance to a surface.<sup>1</sup> Virtually all material objects, especially marine vessels and underwater constructions, are susceptible to biofouling.<sup>2–4</sup> An antifouling coating can downplay the friction and resource wastage caused by biofouling.<sup>5–9</sup> Up to date, a coating cannot suppress the biofouling of a surface completely.<sup>10,11</sup> The transplanted devices often trigger immunogenic responses which result in biofouling.<sup>12,13</sup> This biofouling causes severe infections, killing more than 99,000 people in the United States in 2007.<sup>14</sup> Therefore, a fundamental understanding of antifouling is highly desirable to minimize biofouling.

Marine *mussels* naturally have the unparalleled abilities to deposit adhesive proteins on various surfaces under wet conditions for their survival and self-protection.<sup>15,16</sup> Extensive efforts have been made to mimic the natural adhesives secreted by marine mussels. The strong mussel adhesion is ascribed to *catechol* (1,2-dihydroxybenzene) groups of the mussel adhesive

proteins (MAPs). Elucidating the adhesion mechanism of catechol might provide the key to solving biofouling.

Herein, we investigate whether an electric field reverts the strong adhesion of MAP.<sup>17–19</sup> Specifically, we study the antifouling of catechol adhered onto a hydrophilic silica surface. Previously, the adhesion of catechol onto a silica surface has been studied.<sup>20–24</sup> We apply an external electric field<sup>25</sup> of low strength which is tolerable in the human body. We investigate the effects of such an electric field on the catechol adsorbed on a dry or wet silica surface. By using the *density functional theory* (DFT), we elucidate the molecular-level information on the adhesion and detachment of catechol. We also used an *ab initio* molecular dynamics (MD) simulation to study the dynamics underlying the detachment of catechol induced by an electric field.

## COMPUTATIONAL METHODS

We performed the DFT simulations by using the SIESTA package.<sup>26</sup> We drew the structure of the silica surface

from the bulk structure of  $\text{SiO}_2$  with the tetragonal ( $P4_12_1$ ) symmetry having lattice parameters  $a = b = 4.97 \text{ \AA}$  and  $c = 6.93 \text{ \AA}$ .<sup>27–31</sup> The silica surface was comprised of 16 atomic layers of  $\text{SiO}_2$  and a total number of 198 atoms. The Si and H atoms of the bottom layer of the silica surface were constrained to maintain the bulk structure. We used a large simulation box of  $\sim 40 \text{ \AA}$  in length to remove the art effects of the periodic boundary conditions applied.<sup>27–30,32,33</sup>

We performed the DFT calculations for an isolated catechol molecule, a silica surface, and a catechol molecule adsorbed on the silica surface.<sup>27,30</sup> We modeled the exchange and correlation of electrons by using the generalized gradient approximation (GGA) combined with the revised Perdew–Burke–Ernzerhof (RPBE)<sup>30</sup> functional. The core electrons were treated by using the norm-conserving pseudopotential.<sup>34</sup>

We used the basis set of atomic orbitals with the double zeta with polarizations (DZP) to treat valence electrons. The mesh cut-off was  $2.72 \text{ ke}$ ,<sup>35,36</sup> and the Brillouin zone sampling was done by using  $3 \times 3 \times 1 \text{ k}$  points.<sup>37</sup> All the geometries were fully optimized by using the conjugate gradient method<sup>38</sup> with variable cells. We considered the geometry optimization to be converged when the maximal atomic force was less than  $0.04 \text{ eV/\AA}$ .

We used the semi-empirical method to calculate the dispersion energy proposed by Grimme.<sup>39,40</sup> The Grimme dispersion equation was summed over all possible atomic pairs and considered the two-dimensional periodic boundary condition with the least possible pattern.<sup>41</sup> We used an energy cut-off of  $2721.14 \text{ eV}$  ( $200 \text{ Ry}$ ) for geometry optimization.

We placed an optimized catechol molecule  $3 \text{ \AA}$  above the optimized silica surface. We used the counterpoise correction method to eliminate the basis set superposition error.<sup>42,43</sup>

We ran an ab initio MD simulation by using the GGA and RPBE functionals with the DZP basis set. We ran MD simulations in the NVT ensemble at a human body

temperature ( $330 \text{ K}$ ) with an electrical stimulus of  $2$  or  $20 \text{ V/mm}$ . The time step was  $1 \text{ fs}$ . We used a force tolerance of  $0.04 \text{ eV/\AA}$  in the MD simulation.

## RESULTS AND DISCUSSION

### Adsorption of catechol on a dry or wet silica surface

The optimized geometries of the dry and moist silica surfaces were considered for the adsorption of catechol. Catechol was strongly adhered to the dry or wet surfaces. The optimized geometries of catechol on the dry and wet surfaces are shown in Figure 1a,b, respectively. In Figure 1, the H bonds formed between the surface silanols and the catechol molecule are drawn as the black broken lines. The catechol molecule formed four H bonds with the hydroxyl groups of the dry surface with bond lengths of  $1.74$ ,  $1.73$ ,  $1.93$ , and  $1.82 \text{ \AA}$ . On the wet silica surface, the catechol molecule was surrounded by five water molecules. It formed four H bonds with bond lengths of  $1.82$ ,  $1.849$ ,  $1.69$ , and  $1.77 \text{ \AA}$ .

### Detachment of catechol from surface under an electric field

We applied a human bearable electric field on the catechol molecule adhered to the dry or wet silica surface. The electric field was applied either in the geometry optimization or in the ab initio MD simulation.

In the geometry optimization with an external electrical stimulus, the polarization of the system significantly increased. In contrast, the binding energy of catechol decreased for both the dry and wet surfaces. The bond distance between the molecule on the dry and wet surfaces increased due to the applied field.

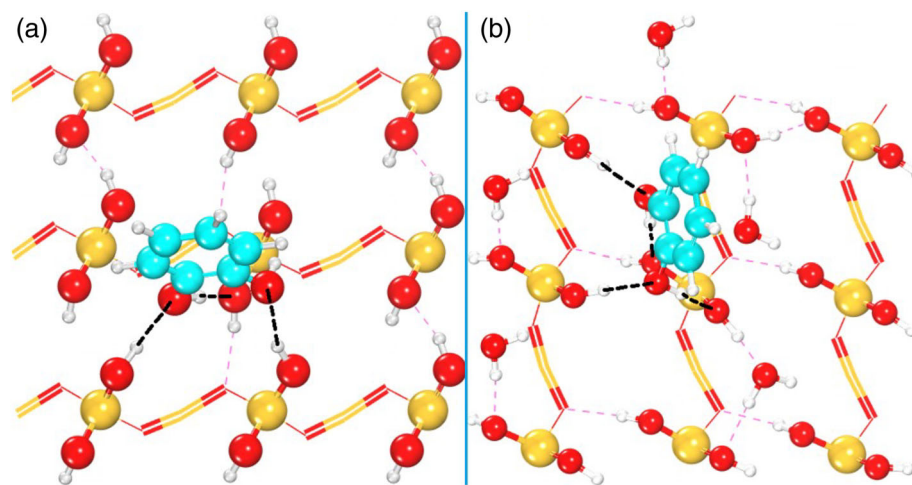


**FIGURE 1** Optimized geometries of catechol molecules adsorbed on the dry (a) and moist (b) silica surfaces. Shown as the orange, red, white, and cyan balls are silicon, oxygen, hydrogen and carbon atoms, respectively. In this and all the following figures, we used the same graphical representation of atoms

In the absence of an electric field, the catechol molecule formed four H bonds with the dry silica surface with bond lengths of 1.74, 1.73, 1.93, and 1.82 Å. With an electrical stimulus of 20 V/mm, these bonds elongated to 1.83, 1.80, 1.96, and 2.21 Å, respectively, as illustrated in Figure 2a. Similarly, with an electric field, the H bonds of catechol adhered to a moist surface also elongated from 1.82, 1.849, 1.69, 1.77 Å to 1.844, 1.956, 1.72, 1.956 Å, respectively (Figure 2b).

Shown in Figure 3 are the variations in the OH bond distances of silanols of the silica surface during the adsorption and desorption of the catechol molecule in the absence and presence of an electric field of 20 V/mm. The black circles represent the O–H bond distances of the silanols on the bare silica surface. Upon adsorption of catechol on the silica

surface, the surface O–H bond distance changed, as drawn as red circles. For the catechol molecule adsorbed on the wet silica, the variations of the bond lengths of the surface silanols (O–H) are drawn as blue circles. With the applied electric field, the surface silanols lengthened in their O–H bond distances because of the increase in the polarization of the silica surface. Overall, the increase in the O–H bond distance was visible in the right of Figure 3. The peaks in the left panel were slightly higher than those in the right panel, indicating the effect of an applied electric field.

In order to estimate the deformations of catechol and surface in the adhesion, we calculated the deformation energy<sup>11</sup> of the catechol molecule  $dE_M$  defined as

$$dE_M = E_{M_S}^m(M) - E_M^m(M),$$

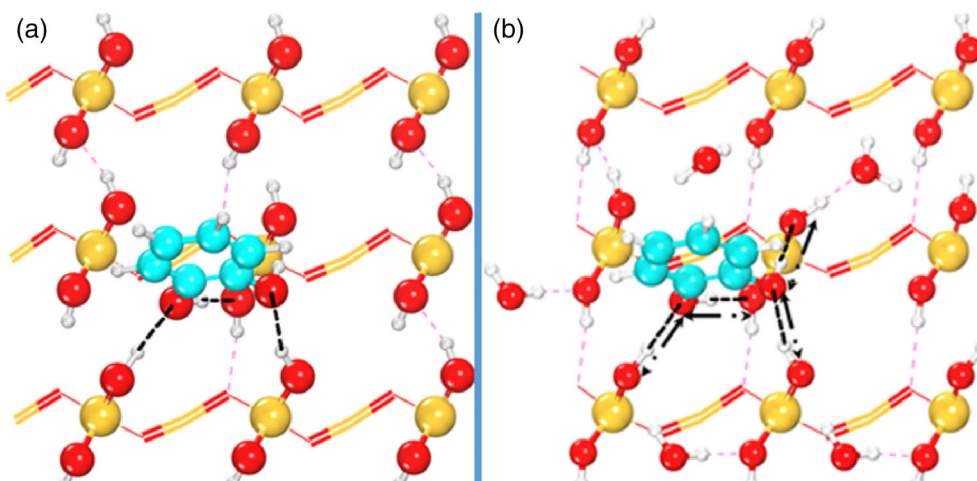


**FIGURE 2** Optimized geometries of the catechol molecules adsorbed on the dry (a) and moist (b) silica surfaces under an applied electric field. The arrows indicate the increases in the distance between molecule and surface

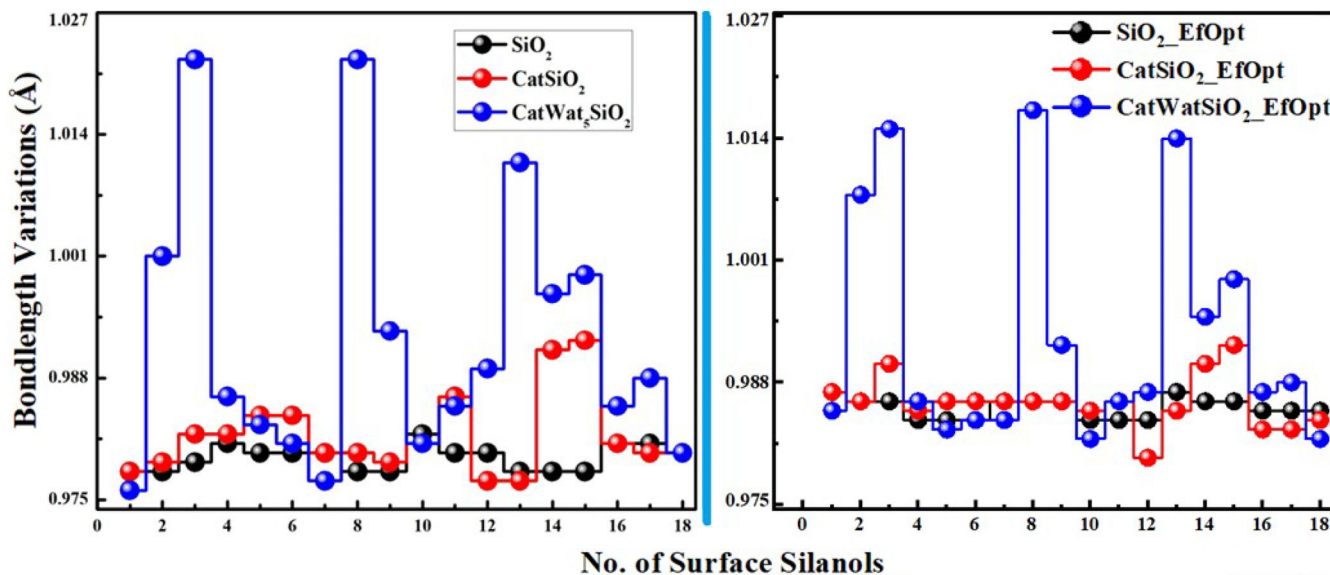


**FIGURE 3** The bond length variation with the number of silanols for catechol in dry and wet environment with zero external electric field (left panel) and non-zero electric field (right panel). The black, red and blue color represents optimized bare silica, catechol adsorbed on dry, and catechol adsorbed surrounded by five water molecules on silica surface, respectively

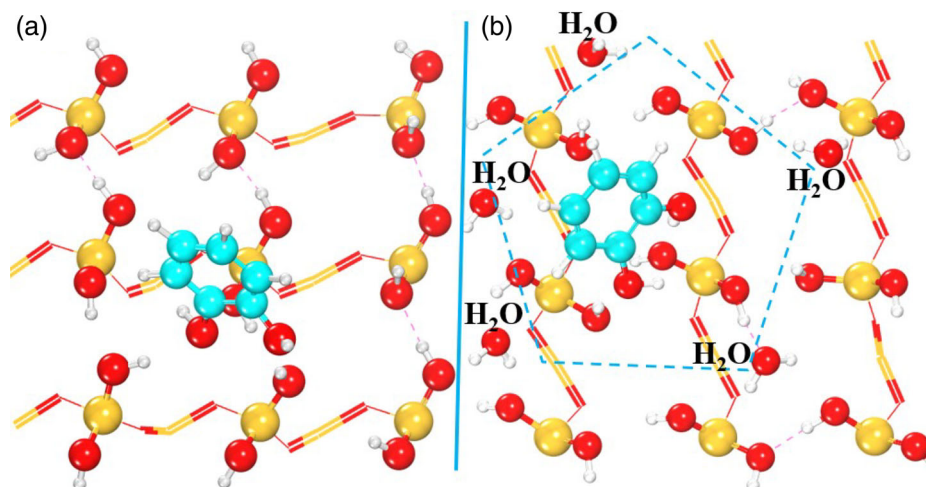


**FIGURE 4** MD simulation of complete detachment of catechol from the surface under an external electric field of 20 V/mm at human body temperature in the dry (a) and wet (b) surfaces. MD, molecular dynamics

and the deformation energy of the surface  $dE_S$  given by

$$dE_S = E_{MS}^s(S) - E_S^s(S).$$

$dE_M$  and  $dE_S$  were found to be 13.26 and 0.84 kcal/mol, respectively. In the presence of an electric field of 20 V/mm, which weakens the molecular adhesion,  $dE_M$  and  $dE_S$  were 4.22 and 3.01 kcal/mol, respectively. After the catechol was electrically detached, the catechol deformed because the adsorption was restored to give  $dE_M$  and  $dE_S$  to 4.22 kcal/mol. In contrast, the  $dE_S$  increased from 0.84 to 3.01 kcal/mol after desorption, signifying the strong adsorption of catechol molecules to the surface.

We ran the ab initio MD simulation to observe the dynamics of the detachment of catechol from the surface in the presence of an electric field. As shown in Figure 4, catechol molecules adhered to the dry and wet surfaces were detached from the surfaces. We observed that the attached catechol molecule visibly rose up from the surface. The catechol molecule was completely detached from both the dry and wet surfaces, showing the adhesion of catechol was completely reversed.

On both the dry and wet surfaces, the polarization of the system significantly decreased, indicating the detachment of molecules from the surface. The silanols of the surface restored their lengths to their initial bond lengths, confirming the detachment of the adhesive molecule from the surface for both the dry and wet surfaces.

Figure 5 shows the binding energies ( $\Delta E$ ) of the catechol adsorbed on the dry and wet silica surfaces without and with an applied electric field of 20 V/mm. The  $\Delta E_s$  calculated from the geometries obtained at the end of the MD simulation are also shown in the figure. One can see that the geometries without electrical stimulus have stronger binding energy than those with electrical stimulus. By applying electrical stimulus to reverse the strongly attached catechol slightly lifted with a slight increase in the bond

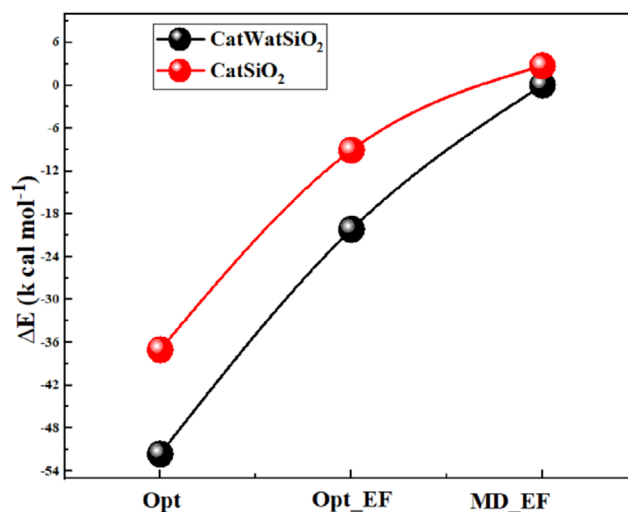


**FIGURE 5** The binding energy of catechol on the dry and wet silica with detachment due to applied electric field which clearly demonstrated that both the molecules were almost detached from the surface

distance with the surface. The MD simulation performed for the detachment purpose clearly established that the molecule is completely reversed from the adsorbed position to almost the position where it was initially placed for the adsorption, that is, 3 Å above the surface.

## CONCLUSION

Catechol plays a central role in the strong adhesion of mussels onto a dry or wet surface. The binding energy of catechol indicates the robust and permanent attachment, which is beneficial for coating purposes. To overcome the problems associated with biofouling, we applied an electrical stimulus of 20 V/mm at human body temperature to



that strongly bonded molecule to reverse this strong attachment. We found that catechol tethered to a silica surface was successfully detached in both dry and wet conditions. Catechol detached from the surface due to an electrical stimulus and lifted from the surface to almost the same position above the surface where it was initially placed. The binding energy and the deformation energy of both molecule and surface confirmed the reversal of the strong adhesion of catechol.

## ACKNOWLEDGMENT

This work was supported by a 2-year Research Grant of Pusan National University.

## CONFLICT OF INTEREST

The authors declare no conflict of interests.

## ORCID

Joonkyung Jang  <https://orcid.org/0000-0001-9028-0605>

## REFERENCES

- [1] M. Al-Bloushi, J. Saththasivam, S. Jeong, A. Al-Refai, R. S. A. Kumar, K. C. Ng, G. L. Amy, T. Leiknes, *Environ. Eng. Res.* **2020**, *26*, 190397.
- [2] V. Vishwakarma, *J. Basic Microbiol.* **2020**, *60*, 198.
- [3] A. V. Samrot, A. Abubakar Mohamed, E. Faradjeva, L. Si Jie, C. Hooi Sze, A. Arif, T. Chuan Sean, E. Norbert Michael, C. Yeok Mun, N. X. Qi, P. L. Mok, S. S. Kumar, *Medicina* **2021**, *57*, 839.
- [4] E. Arzt, H. Quan, R. M. McMeeking, R. Hensel, *Prog. Mater. Sci.* **2021**, *119*, 100823.
- [5] A. M. Maan, A. H. Hofman, W. M. de Vos, M. Kamperman, *Adv. Funct. Mater.* **2020**, *30*, 2000936.
- [6] S. Tian, D. Jiang, J. Pu, X. Sun, Z. Li, B. Wu, W. Zheng, W. Liu, Z. Liu, *Chem. Eng. J.* **2019**, *370*, 1.
- [7] L. Shamaei, B. Khorshidi, M. A. Islam, M. Sadrzadeh, *J. Cleaner Prod.* **2020**, *256*, 120304.
- [8] Y. Jeong, S. M. Kang, *Bull. Korean Chem. Soc.* **2020**, *41*, 1068.
- [9] S. Kim, Y. Jeong, S. M. Kang, *Bull. Korean Chem. Soc.* **2016**, *37*, 404.
- [10] C. I. Idumah, C. M. Obele, E. O. Emmanuel, A. Hassan, N. Azikiwe, *Surf. Interfaces* **2020**, *21*, 100734.
- [11] M. U. Farid, N. K. Khanzada, A. K. An, *Desalination* **2019**, *456*, 74.
- [12] Q. Liu, A. Chiu, L. Wang, D. An, W. Li, E. Y. Chen, Y. Zhang, Y. Pardo, S. P. McDonough, L. Liu, *Biomaterials* **2020**, *230*, 119640.
- [13] O. J. Uwaezuoke, P. Kumar, V. Pillay, Y. E. Choonara, *Drug Deliv. Transl. Res.* **2021**, *11*, 1903.
- [14] Emergency Severity Index: A Triage Tool for Emergency Departments, <https://www.ahrq.gov/professionals/systems/hospital/esi/index.html> (accessed: 2018).
- [15] X. Zhang, Q. Lu, Z. Ding, W. Cheng, L. Xiao, Q. Lu, in *Injectable Hydrogels for 3D Bioprinting*, Vol. 8 (Eds: I. Noh, X. Wang, S. van Vlierberghe), Royal Society of Chemistry, Croydon, UK **2021**, p. 155.
- [16] M. K. Islam, P. J. Hazell, J. P. Escobedo, H. Wang, *Mater. Des.* **2021**, *205*, 109730.
- [17] S. Mian, S. Azzam, G. Rahman, *MOJ Biorg. Org. Chem.* **2017**, *1*, 211.
- [18] M. N. George, E. Carrington, *Biofouling* **2018**, *34*, 388.
- [19] T. Priemel, R. Palia, M. Babych, C. J. Thibodeaux, S. Bourgault, M. J. Harrington, *Proc. Natl. Acad. Sci. U. S. A.* **2020**, *117*, 7613.
- [20] W. Zhang, R. Wang, Z. Sun, X. Zhu, Q. Zhao, T. Zhang, A. Cholewinski, F. K. Yang, B. Zhao, R. Pinnaratip, *Chem. Soc. Rev.* **2020**, *49*, 433.
- [21] A. H. Hofman, I. A. van Hees, J. Yang, M. Kamperman, *Adv. Mater.* **2018**, *30*, 1704640.
- [22] S. Moulay, *Orient. J. Chem.* **2018**, *34*, 1153.
- [23] J. Saiz-Poseu, J. Mancebo-Aracil, F. Nador, F. Busqué, D. Ruiz-Molina, *Angew. Chem., Int. Ed.* **2019**, *58*, 696.
- [24] E. E. de Moraes, M. Z. Tonel, S. B. Fagan, M. C. Barbosa, *J. Mol. Model.* **2019**, *25*, 302.
- [25] A.-K. Petri, K. Schmiedchen, D. Stunder, D. Dechent, T. Kraus, W. H. Bailey, S. Driessen, *Environ. Health* **2017**, *16*, 41.
- [26] E. Artacho, J.M. Cela, J.D. Gale, A. García, J. Junquera, R.M. Martin, P. Ordejón, N.R. Papior, D. Sánchez-Portal, J.M. Soler, SIESTA 4.1-b4, **2018**.
- [27] S. A. Mian, L.-M. Yang, L. C. Saha, E. Ahmed, M. Ajmal, E. Ganz, *Langmuir* **2014**, *30*, 6906.
- [28] S. A. Mian, L. C. Saha, J. Jang, L. Wang, X. Gao, S. Nagase, *J. Phys. Chem. C* **2010**, *114*, 20793.
- [29] S. A. Mian, Y. Khan, *J. Chem.* **2017**, *2017*, 8756519.
- [30] S. A. Mian, Y. Khan, U. Ahmad, M. A. Khan, G. Rahman, S. Ali, *RSC Adv.* **2016**, *6*, 114313.
- [31] A. Rimola, S. Tosoni, M. Sodupe, P. Ugliengo, *ChemPhysChem* **2006**, *7*, 157.
- [32] M. Corno, M. Delle Piane, P. Choquet, P. Ugliengo, *Phys. Chem. Chem. Phys.* **2017**, *19*, 7793.
- [33] S. K. Singh, A. Parashar, *Eng. Fract. Mech.* **2021**, *243*, 107536.
- [34] J.-B. Lu, D. C. Cantu, C.-Q. Xu, M.-T. Nguyen, H.-S. Hu, V.-A. Glezakou, R. Rousseau, J. Li, *J. Chem. Theory Comput.* **2021**, *17*, 3360.
- [35] G. R. Schleder, A. C. M. Padilha, A. Reily Rocha, G. M. Dalpian, A. Fazzio, *J. Chem. Inf. Model.* **2019**, *60*, 452.
- [36] P. Pollak, F. Weigend, *J. Chem. Theory Comput.* **2017**, *13*, 3696.
- [37] H. Felipe, D. Y. Qiu, S. G. Louie, *Phys. Rev. B* **2017**, *95*, 035109.
- [38] A. A. Al-Arbo, R. Z. Al-Kawaz, *Indones. J. Electr. Eng. Comput. Sci.* **2021**, *21*, 429.
- [39] C. Bannwarth, S. Ehlert, S. Grimme, *J. Chem. Theory Comput.* **2019**, *15*, 1652.
- [40] E. Caldeweyher, S. Ehlert, A. Hansen, H. Neugebauer, S. Spicher, C. Bannwarth, S. Grimme, *J. Chem. Phys.* **2019**, *150*, 154122.
- [41] S. Grimme, C. Bannwarth, E. Caldeweyher, J. Pisarek, A. Hansen, *J. Chem. Phys.* **2017**, *147*, 161708.
- [42] B. G. Peyton, T. D. Crawford, *J. Phys. Chem. A* **2019**, *123*, 4500.
- [43] J. Witte, J. B. Neaton, M. Head-Gordon, *J. Chem. Phys.* **2017**, *146*, 234105.

**How to cite this article:** M. Ilyas, S. A. Mian, A. Rauf, E. Ahmed, G. Rahman, A. Sannyal, J. Jang, *Bull. Korean Chem. Soc* **2022**, *43*(2), 210. <https://doi.org/10.1002/bkcs.12454>